STRUCTURAL STABILITY IN PHYSICS:

RECENT TRENDS AND PROBLEMS*

Werner Güttinger
Institute for Information Sciences
University of Tübingen
Tübingen, Fed. Rep. of Germany

Dedicated to Mario Schönberg on the occasion of his 70th birthday

SUMMARY

It is shown that the topological singularities and bifurcation processes deriving from the concept of structural stability determine the most significant phenomena observed in both structure formation and structure recognition. From this emerges a comprehensive and unifying theoretical framework for the description of nonlinear physical systems which, when passing through instabilities, exhibit critical and analogous behavior. The basic concepts of singularity and bifurcation theory are outlined and applied to a variety of fields. These include the inverse scattering problem, nonlinear phonon focusing, interacting spatio-temporal patterns, optical bistability, and critical phenomena in condensed matter and particle physics. An outlook is given on future developments.

*Research supported by the Stiftung Volkswagenwerk, F.R.G.

TABLE OF CONTENTS

I. INTRODUCTION

The increasing diversification of the physical sciences during recent years and the complexity of observed phenomena have made it more and more imperative to search for unifying physical principles. These reveal themselves in a wealth of fascinating analogies discovered in the critical behavior of dynamical systems of various genesis which, when passing through instabilities, suddenly exhibit new spatio-temporal patterns or modes of behavior.

The phenomenological picture looks indeed seductively general. There is a striking similarity among the instabilities that lead to convection patterns in fluids, cellular solidification fronts in crystal growith, geophysical textures, vortex formation in superconductors, phase transitions in condensed matter and particle physics, biological and chemical patterns or rhythms, and so forth. Many of these systems are extremely interesting for scientific and technological as well as aesthetic reasons. Their common characteristic is that one or more significant behavior variables or order parameters

undergo spontaneous, large and discontinuous changes or cascades of these if slow, competing but continuously driving control parameters or forces cross a bifurcation set and enter conflicting regimes. As a consequence, an initially quiescent system becomes unstable at a critical value of some control variable and then restabilizes into a more complex space- or time-dependent configuration. Primary bifurcations induce limit cycles, spatial patterns and spatio-temporal patterns in the form of standing waves when the bifurcation branches remain disjoint. If other controls cause these branches to interact, multiple degenerate bifurcation points produce higher instabilities. Then the system undergoes additional transitions into more complex states, giving rise to traveling waves, hysteresis, resonance and entrainment effects. These ultimately lead to states which are intrinsically chaotic. In the vicinity of degenerate bifurcation points a system becomes extremely sensitive to small ambient factors like imperfections, external fields or fluctuations that lead to symmetry breaking. This in turn

enhances the system's ability to perceive its external environment and, adapting to it by capturing its asymmetry, to form preferred patterns or modes of behavior. Most prominent among the theoretical programs venturing into the area of general principles are Prigogine's concept of dissipation structures [1], Haken's synergetics [2] and Thom's catastrophe theory [3]. Among these Thom's program has both the potential to provide a geometrical explanation for the variety of analogies encountered in the critical behavior of systems of different genesis and, as we shall show, also the power to predict new phenomena.

Nature surprises us with the fact that the tremendous amount of physical data and results can be condensed into a few simple laws that summarize our knowledge. These laws are essentially qualitative. In mathematical terms "qualitative" means not "poorly quantitative" but topologically invariant, i.e., independent of a coordinate description. Common to analogous critical physical phenomena, besides their

qualitative similarity, is their universality expressed by the fact that the details of the interaction of a system undergoing spontaneous transitions are often almost irrelevant. This calls for a topologically invariant description of the phenomena under consideration. When Feynman discussed turbulence he observed that "the next great era of awakening of human intellect may well produce a method for understanding the qualitative content of complex equations." R. Thom has undoubtedly opened the door to it.

The basic role physics plays in the sciences may be traced to the fact that most systems and structures in nature enjoy an inherent physical stability properly: They preserve their quality under slight perturbations, i.e., they are structurally stable. Otherwise we could hardly think about or describe them, and today's experiment would not reproduce yesterday's results. We do not know how it got that way. But accepting structural stability as a fundamental principle, universal critical physical phenomena have a common

topological origin. They are describable and classifiable by stable unfoldings of singularities of smooth maps, i.e., in terms of topological normal forms that act as organizing centers for the bifurcation processes exhibited by dynamical systems of various genesis. We use the term bifurcation to refer to changes in the qualitative structure of solutions to differential equations. A phenomenon is said to be structurally stable if it persists under all allowed perturbations in the system. Most of the nonlinear equations of physics are not amenable to a quantitative analysis and few, if any, are completely known, so that it is often not clear for which particular effects one ought to look. Since they derive from geometrical invariance principles and conservation laws they must possess structurally stable solutions. To determine these provides us with conceptual guidance to single out the most significant phenomena and to answer the basic questions of structure formation and structure recognition which we address in this paper: (i) How do structures emerge from a structureless environment and how can we classify the transitions between the hierarchy of possible

configurations? (ii) How do we recognize and reconstruct unknown structures from complex recorded data and how can we classify and interprete them? (ii) is the inverse problem of (i). Since the evolution of structures is intrinsically tied to a recognition and adaptation process, and since both are geometric phenomena, uncovering their common topological roots raises very difficult but fascinating questions that promise a great challenge for future research.

In pursuing the goal of a geometrization of physics I begin with a review of the basic principles of singularity and bifurcation theory and then apply them to a variety of problems in structure formation and structure recognition both at the microscopic and macroscopic levels. I have tried to make the various chapters self-contained and to reflect the actual situation in this field of research. However, there is no attempt at completeness, neither in coverage nor in references.

II. STRUCTURAL STABILITY, SINGULARITIES AND BIFURCATIONS

1. Structural Stability

In this section we outline the basic principles of singularity and bifurcation theory, referring to [4]-[7] for further details. A physical system is said to be structurally stable if it preserves its quality under slight distortions. In particular, a nonlinear dynamical system $\dot{\underline{x}}(t)=\underline{F}(\underline{x},\lambda)$, $\underline{x}\in R^n$, $\lambda\in R$, is structurally stable if the phase portrait of the perturbed system $\dot{\underline{x}}=\underline{F}+\underline{\delta}$ is topologically equivalent to that of the unperturbed system. Since in a structurally stable system nothing new happens when it is perturbed, we are interested in unstable systems whose perturbation gives rise to new modes of behavior. Bifurcation occurs in a parametrized dynamical system when a variation of a parameter causes a qualitative change in the behavior of solutions, e.g., when an equilibrium splits into two. Catastrophe occurs when the stability of an equilibrium breaks down, causing the system to jump into another state.

The pitchfork bifurcation provides a familiar example. The stationary states $\dot{x}=0$ of the system $\dot{x}=G\equiv x^3-\lambda x$ can be represented by the bifurcation diagram of Figure 1. The trivial solution branches at the bifurcation point ($x=0$, $\lambda=0$) which is a singularity of G. The bifurcation diagram of the Hopf bifurcation of a periodic solution from a stationary one follows from Figure 1 by rotating the parabola around the λ-axis above a (x,y)-plane with y orthogonal to (x,λ). Introducing polar coordinates r,θ in the (x,y)-plane the canonical equations are $\dot{\theta}=1$, $\dot{r}=-(r^3-\lambda r)$. When $\lambda<0$, the origin is an attractor (all trajectories spiral into it); when $\lambda>0$, the radial component is outward for $r<\sqrt{\lambda}$ and inward for $r>\sqrt{\lambda}$; the origin becomes a repellor and there is a stable limit cycle thrown off with $r=\sqrt{\lambda}$. The point $\lambda=0$ is a Hopf bifurcation point, the amplitude grows on a paraboloid and the origin is an organizing center for the singularity.

A bifurcation problem consists of the solution of a system of equations $G(x,\lambda)=0$ with $G(0,0)=0$, $d_xG(0,0)=0$ where G is a germ of a C^∞ mapping of $R^n\times R$ into R^m. The point ($x=0$, $\lambda=0$) is called a bifurcation point or a singularity of G. This does not necessarily mean that solutions $x(\lambda)$ branch at the bifurcation point but merely implies that the solution diagram changes its qualitative form under small perturbations of G. For example, a hysteresis point, i.e., a point where the solu-

tion has a vertical tangent, is a bifurcation point since an appropriate perturbation changes the solution type from a monostable to a bistable one. At a bifurcation point a system becomes structurally unstable. The main result of singularity theory is that, in the course of possible bifurcations, a system does not become unstable in an arbitrary way. Instead, the bifurcations occur in certain definite and indeed classifiable ways. Consequently, a structurally unstable event can be embedded into a structurally stable family of maps or systems. This family is parametrized by a number of unfolding or control parameters. The number of parameters that is necessary to embed a given bifurcation into a stable family is called the codimension of the bifurcation or singularity. Thus, a structurally unstable event may occur within a structurally stable process.

2. Catastrophe Theory

Thom's "elementary catastrophe theory" [3] provides the basis for what is now called topologically invariant bifurcation theory. It can be thought of as describing the stable bifurcations of the stationary states of a gradient system

$\dot{x}_i = \partial f(x,a)/\partial x_i$ with $x=(x_1,\ldots,x_n)\in R^n$ when the parameters $a=(u,v,w,\ldots)\in R^k$ in the "potential" function $f:R^n \times R^r \to R$ vary. Catastrophe theory deals with the classification of degenerate singular points of smooth real-valued, parametrized families of functions of n real variables. The singular points of a smooth function $f:R^n \to R$ are the points x where the differential vanishes: $(df)(x)=\text{grad } f(x)=0$. The function f has a nondegenerate (or Morse) singularity at x if the second differential $(d^2f)(x)=(\partial^2 f(x)/\partial x_i \partial x_k)$ is a nondegenerate quadratic form, i.e., if the Hessian $H(x)=\det(d^2f)$ does not vanish. Using suitable local coordinates, the function f can in some neighborhood of a nondegenerate singular point be represented in the Morse normal form $f=\text{const} + \Sigma(\pm x_i^2)$. Morse singularities are stable in the sense that a small perturbation g of f (with g, dg, d^2g near f, df, d^2f) also has a Morse singularity. On the other hand, every degenerate singular point x of f, for which H=0, bifurcates into some nondegenerate points after an arbitrarily small deformation. The function $f(x)=x^3/3 (x\in R)$ and its perturbation $f_t(x)=x^3/3+tx$ furnish a familiar example. We see that degenerate singular

points appear naturally if the function depends upon parameters, i.e., if one considers not an individual function but a parametrized family of functions. Then it is possible for a non-Morse function to appear as a member of a "stable family". In the above example, $f=x^3/3$ is not stable at $x=0$ because a small perturbation of it, generated by adding tx, radically changes its shape when t is varied: for $t<0$, $f_t(x)$ has two extrema while for $t>0$ it has none. Thus, the family $f_t(x)=x^3/3+tx$ is stable as a (t-)parametrized family near $x=0$. We call $f_t(x)$ the unfolding of f, t an unfolding parameter, and $t=0$ a catastrophe point of the family because it separates the stable regions $t\lessgtr 0$. Formally, one may continue playing by considering the function $f=x^4/4$, $x\in R$, and its unfolding (or perturbation) $f_{uv}(x)=x^4/4+ux^2/2+vx$ near its singularity $x=0$. The singular points are given by an overhanging cliff S, Figure 2, given by $f'_{uv}(x)=x^3+ux+v=0$, in (x,u,v)-space, and projecting the tangents (parallel to x) of its two edges, given by $f''_{uv}=3x^2+u=0$, vertically onto the (u,v)-plane by eliminating x from the two equations, one obtains the familiar cusp equation $B: 4u^3+27v^2=0$, viz., the bifurcation set of Fig. 3

on which two stationary points (a minimum and a maximum) of f_{uv} coalesce.

We have embedded f into the unfolding f_{uv}. While f is a very fragile object because its singularity is degenerate, the shapes of f_{uv} remain basically the same inside or outside the cusp, respectively (two minima of f_{uv} if u and v vary inside B, one minimum of f_{uv} if u and v stay outside of B): f_{uv} remains stable under small variations of (u,v) not crossing B. B is a singularity of the map of S onto the plane made up by (u,v). Intuitively, deforming S smoothly does not change the qualities of the "cusp catastrophe". Take a two-dimensional manifold $M\subset R^3$. Lift it into R^3, deform it as you please and map it vertically down onto R^2. You will discover four sorts of points on the fiber M: (a) regular points which lie smoothly over R^2, singular points, i.e., some on the edges of folds (b), and some marking the origin of an overhanging cliff (c), and, finally, (d) points which resemble none of the former. Deform the fiber slightly near any of these points. A bit of experimentation shows the following: The location of points of type (a), (b), and (c) will be shifted a bit

but their "quality" remains the same and they cannot be made to disappear under such small deformations of the fiber. But all the messy points of type (d), or worse, turn under small deformations into points of type (a), (b) or (c). This is an experimental "proof" of the Thom-Whitney theorem: Consider the space F of all 2-parameter families of functions $f(x;\alpha,\beta)$ and their singularities $df=0$. Call $f\in F$ structurally stable if it has a neighborhood of equivalents. Then the only singularities of the projection $M\to R^2$ are folds and cusps. This means that the most complicated behavior that can happen locally is the cusp. While this is a geometric fact, its physical meaning is obvious: If a system with one behavior variable or order parameter x is slowly driven from one phase to another by a control variable v, and if an orthogonal drive u sets in to split the quality of the phases (different states of order or symmetry, etc.) and if a phase may persist for a while with the transition to the other delayed, then the cusp catastrophe is intuitively the simplest model and, as we have seen, the least fragile.

Catastrophe theory classifies the singularities of maps $f:R^n\to R$ into equivalence classes. Two functions f and g in the same class are called (right-) equivalent if $f(x)=g(\phi(x))+\text{const}$, where ϕ is a diffeomorphism. Functions from different classes differ by the number of control or unfolding parameters a and by the form of the unfolding terms which have to be added to a function in order to embed the degenerate singular point into a stable family. The number of terms is the codimension of the singularity of f. Then Thom's theorem states: Let $f:R^n\times R^r\to R$ be a parametrized family of smooth functions $f_a:R^n\to R$, where $a\in R^r$. Let $r\leq 3$, $a=(u,v,w)$, $(x_1,x_2,\ldots)=(x,y\ldots)$. Then almost all such f are (up to the addition of a Morse function) equivalent to a function $P(x,a)$ out of the following list: $[A_2]$: $P=x^3+ux$ (fold); $[A_3]$: $P=x^4+ux^2+vx$ (cusp); $[A_4]$: $P=x^5+ux^3+vx^2+wx$ (swallowtail); $[D_4^+]$: $P=x^3+xy^2+uy^2+vx+wy$ (hyperbolic umbilic); $[D_4^-]$: $P=xy^2-x^3+ux^2+uy^2+vx+wy$ (elliptic umbilic). The list can be extended to $r>3$ [8]. The polynomials $P(x,0)$ are called normal forms of the singularities and the associated families $P(x,a)$ are their unfoldings. We denote by $M=\{(x,a)\,|\,df(x,a)=0\}$ the catastrophe

manifold of f. $\Sigma=\{(x,a)\,|\,df=0,\ \text{Det}\ d^2f=0\}$ is the singularity set, where Det d^2f is the Hessian of f. The projection $\chi: M \to R^r$ of M on the bifurcation set $B=\{a\,|\,(x,a)\in\Sigma \text{ for } x\in R^n\}$ gives the familiar Thom diagrams of Figs. 3-6. When a varies transversely through B, the topology of the extrema of f changes in a neighborhood of the origin. We shall show below, in a physical context, that catastrophe theory classifies surface evolutes (Sec. III).

3. Imperfect Bifurcations

Bifurcation is, in a sense, an idealized, nongeneric phenomenon: diagrams such as the pitchfork in Figure 1 are structurally unstable, and small perturbations of the mapping will break the bifurcation diagram. The two branches of the pitchfork may, e.g., be interpreted as the primary right or left displacements of an elastic vertical column buckling under a load λ. Also the two branches may represent the two magnetization directions in a ferromagnet below critical temperature. Since imperfections are present in any physical system we should require that a description of the transition point include the effects of variations (impurities, imperfections etc.) in the problem other than the distinguished bifurcation parameter. If the idealized bifurcation problem is determined by $G(x,\lambda)=x^3-\lambda x=0$, for example, what is the most general form of the solution structure under small perturbations of the system? Golubitsky and Schaeffer [9] have addressed this question using the theory of singularities of mapping which goes under the name of imperfect bifurcation theory and generalizes Thom's theory.

Consider a bifurcation problem

$$G(x,\lambda) = 0 \qquad (2.1)$$

with $d_xG(0,0) = 0$, where $G: R^n \times R \to R^m$, $x\in R^n$, and $\lambda\in R$ is a distinguished, externally controllable bifurcation parameter -- distinct from others describing perturbations -- which represents the control variable in a physical experiment. We may, for example, assume that (2.1) is the equation for the amplitudes x of the solutions of a system of nonlinear evolution equations $\partial u/\partial t=F(u,\lambda)$ obtained by a Lyapunov-Schmidt reduction (Sec. IV). In [9] a technique has been developed which permits the determination of all possible qualitatively different bifurcation diagrams in a neighborhood of the singularity $(x=0,\ \lambda=0)$

which are stable against perturbations of G by changing coordinates in such a way that G reduces to polynomial normal forms. The reduction of a system of evolution equations to an algebraic system (2.1) is not unique and the possibility arises that two bifurcation problems G and G' assume different forms although they possess qualitatively the same solutions. We call G and G' contact equivalent if there exists a smoothly parametrized family of invertible matrices $T(x,\lambda)$ on R^m and diffeomorphisms $x \to X(x,\lambda)$, $\lambda \to \Lambda(\lambda)$ such that

$$G'(x,\lambda) = T(x,\lambda)\cdot G(X(x,\lambda),\Lambda(\lambda)) \qquad (2.2)$$

The distinghuished parameter λ is not allowed to mix with the order parameters or state variables x. The topology of the bifurcation diagram $B(G)=\{(x,\lambda)\,|\,G=0\}$ remains invariant under (2.2) relative to the λ-coordinate. A typical example is this: Let $G(x,\lambda)$ be a bifurcation problem such that at $x=\lambda=0$ we have $G=G_x=G_{xx}=G_\lambda=0$ and $G_{xxx}G_{x\lambda}<0$. Then G is contact equivalent to the pitchfork $x^3-\lambda x$.

To characterize all perturbations of G which respect the special role of λ amounts to finding a universal unfolding and then enumerating all qualitatively distinct bifurcation

diagrams. Their number is called the codimension of G. Denoting a perturbation of G by $G_\alpha=G+H_\alpha$ with a perturbation term H_α with $H_o=0$, we call the unfolding parameters imperfection parameters. G_α is a stable unfolding of G if, for any other unfolding G_β, there exists a smooth map $\alpha=\psi(\beta)$ such that $G_{\psi(\beta)}$ is contact equivalent to G_β. G_α is universal if it is stable and possesses the minimum number of unfolding parameters needed for stability. With these definitions we have the following theorem [9]: A bifurcation problem of finite codimension is contact equivalent to one described by polynomial normal forms whose universal unfoldings are also polynomials. The list of normal forms presently known is, however, not yet as complete as is the Thom-Arnold list. As an example we show in Figure 7 a typical bifurcation diagram for the perturbed pitchfork with universal unfolding $G_\alpha=x^3-\lambda x+\alpha_1 x^2+\alpha_2$. The imperfect bifurcation theory outlined above has been generalized to problems with symmetry [10]. Let G be a bifurcation problem with m=n and Γ a compact Lie group acting orthogonally on R^n. Then G is a bifurcation problem with symmetry group Γ if for all $\gamma\in\Gamma$ we have $G(\gamma x,\lambda)=\gamma G(x,\lambda)$. One has

then to analyse the problem in which a perturbation breaks symmetry. Stable ways to break symmetry in the pitchfork seem to be obvious but a general theory of symmetry breaking is still missing [10],[11].

In a given physical system different types of bifurcations may occur which interact when λ reaches a critical value (Sec. IV). In addition, in many instances only partial information about the system's behavior is available. It is therefore pertinent to ask if a highly singular configuration, an "organizing center" [12], can be found, in which all singularities are pushed together in such a way that its unfoldings not only reproduce the experimentally established bifurcations but also bridge the gap between these in the sense that different sections through the space of unfolding parameters reveal new stable bifurcations which have so far not been observed. To achieve this the following definition of an organizing center is invoked: Let G and G' be bifurcation problems and let G_α be a stable unfolding of G. To any set $\mu=(x_o,\lambda_o,\alpha)$ such that $G_\alpha(x_o,\lambda_o)=0$ we associate a bifurcation problem defined by

$$G_\mu(x,\lambda) = G_\alpha(x_o+x,\lambda_o+\lambda).$$

Then G is called an organizing center of G' (i.e., G organizes G') if there is a μ such that G_μ is contact equivalent to G'. The geometrical meaning of the organizing center of a normal form is the following. G is an organizing center of G' if the bifurcation diagram of G' appears as a subdiagram of the universal unfolding of G for some value of the unfolding parameter α. This is to say that the bifurcation diagram of G_α is qualitatively the same as that of G'. Consequently, the singularities of G' are compressed into one highly singular configuration of G whose perturbation reveals all possible imperfection effects. Such organizing centers have been found in thermal chainbranching models [13], in the Hodgkin-Huxley model of neurons [14] and in optical bistability [15] (cf. Sec. IV). In these cases the critical value λ_o of the organizing center usually lies outside the physical region. So one might wonder if, for example, in cosmology time values before the big bang are relevant for the expansion of the universe.

4. Applications

The concepts of singularity and bifurcation theory discussed above have given rise to a wealth of applications in the

physical sciences [4]-[7] and provide the topological bones on which to sew the dynamical flesh of nonlinear evolution equations [35]-[37]. Without entering the latter field [42] we conclude this section with a few applications which illustrate our general considerations.

(i) Nonlinear Conservation Laws. Consider the quasilinear wave equation

$$\psi_t + q_x(\psi) = \psi_t + c(\psi)\psi_x = 0 \qquad (2.3)$$

for the amplitude $\psi(t,x)$, t being the time and $x\in R$, with initial condition $\psi(x,o)=f(x)$. The solution of (2.3) is given implicitly by $F(\psi):=\psi-f(x-c(\psi)t)=0$. Suppose that $c'(\psi)>0$. Then larger amplitudes propagate faster along the x-axis than lower ones and, if $f'<0$ on some section of the x-axis, one sees from $F'=0$ that the wave starts to break at a critical time t_c. Consequently the shape of the wave is given by the catastrophe manifold S of Figure 2 with the identification $(x,u,v)\to(\psi,-t,x)$. The cusp in the (u,v)-plane is the envelope of the characteristics of (2.3). If $x\in R^3$, the only singularities the wave motion can exhibit are folds,

cusps and butterfly catastrophes. This model serves as a basis for Zeldovich's theory of the large scale distribution of matter in the universe. When one asks for a single-valued but discontinuous solution ψ of (2.3), the Rankine-Hugoniot (RH) jump condition $s\cdot[\psi]=[q]$ must be invoked where $s=\dot{x}$ is the speed of the discontinuity and [g] the jump of g across that line (Maxwell convention). (2.3) also describes two phases in equilibrium thermodynamics when the volume V is kept constant. In this case $\psi=V$, q is the entropy, t the temperature, x the pressure and the RH condition becomes the Clausius-Clapeyron formula. In mechanics, the Hamiltonian H satisfies (2.3) if we identify $(t,x,\psi,c)=(p,q,H,-\partial_H J)$ where J is the action J(q,H). Then the RH condition reads $(H_2-H_1)/(J_2-J_1)=dp/dq\equiv\nu$. If we assume that $J_2-J_1=h$, the RH condition is nothing but the Ritz combination principle. Returning to cosmology, it is likely that the geometric nature of phase transitions in gauge theories and problems of the inflationary universe may be captured by singularity and bifurcation theory. We shall discuss these problems elsewhere [16].

(ii) Topological versus Analytical Singularities. Let $f(x,\lambda)=0$ define a parametrized hypersurface S in R^n. Then the well-known formula

$$I(\lambda) := \int_{R^n} \delta(f(x,\lambda))\psi dx = \int_{S:f=0} \frac{dS\ \psi}{|\nabla f(x,\lambda)|} \qquad (2.4)$$

(with a smooth $\psi(x)$) establishes a relation between the topological singularities of f ($\nabla f=0$ where the integrand is largest) and the analytical singularities $I(\lambda)$ will possess at values of λ for which both f and ∇f vanish. We shall see in Sec. III that this is at the origin of some problems encountered in the inverse scattering and phonon focusing. Here we wish to illustrate the significance of Equ. (2.4) in other fields of physics in virtue of the classification of imperfect bifurcation problems discussed in Sec. II.3.

(1) Crystal spectra: Consider a vibrating system with a dispersion relation $\omega=\omega(k)$. Then, with f in (2.4) replaced by $\omega(k)$, Equ. (2.4) represents the distribution function for the density of modes. In the Morse case this gives rise to van Hove singularities, in the degenerate case one can classify the spectra by means of the normal forms governing

imperfect bifurcation theory. The same argument applies to the density of orbitals in an electron plasma, to the problem of band structures in semiconductors and to magnon interactions [17]. (2) Dispersive wave phenomena: In a dispersive medium with a time-harmonic source with frequency ω and a dispersion relation $f(\omega,\underline{k})=0$, I is the wave function at point $\underline{x}$, $\psi=\exp(i\underline{k}\underline{x})$ and the integral goes over the surface S_ω in $\underline{k}$-space defined by f=0. Imperfect bifurcation theory yields then readily a classification for the bifurcation modes of waves in a dispersive medium [18], [17].

(iii) Particle Physics. Analysing phase transitions in particle physics and cosmology, and symmetry breaking in gauge theories from the point of view of bifurcation theory are presently in the center of interest [16]. Phase transitions in flavor QCD are equivalent to pitchfork bifurcations and their unfoldings. Breaking SUSY may correspond to unfolding the double-cusp.

III. TOPOLOGICAL SINGULARITIES AND WAVE MOTION

Wave systems provide a tool for the investigation of unknown structures. Thus the question arises, what information about that structure can be inferred from the singularities which it impresses upon a sensing wavefield. Imposing the principle of structural stability -- i.e., qualitative insensitivity to slight perturbations -- on this "inverse scattering problem", we show that, because of the overall space-time view this topological approach permits, the complex high-intensity patterns in the output recordings can be reduced to a few universal standard forms. These are the only ones an unknown object or medium can generically impress upon a sensing wave system. This view of the inverse scattering problem generalizes classical S-matrix theory in the sense that the observed singularities in scattering amplitudes and cross-sections are linked with the topological singularities of the scatterer. Since the latter can be classified, so can the former, and a new structural approach to the inversion problem emerges.

We confine ourselves to the discussion of two problems, viz. remote sensing of layered media and phonon focusing in condensed matter physics. The central idea underlying this geometrical approach is the following. In order that the reconstruction of surfaces and subsurface structures from backscattered or transmitted waves be physically feasible, i.e., repeatable, the scattering process underlying remote sensing has to be structurally stable, i.e., qualitatively insensitive to slight perturbations of the sensing wave system. Otherwise today's experiment would not reproduce yesterday's result. Imposing the principle of structural stability on the inversion process has the following consequences. It permits us to classify the geometric singularities that an unknown surface or structure generically impresses on a sensing wavefield into a few universal topological normal forms described by catastrophe polynomials. These geometrical singularities produce the dominant analytic singularities and typical configurations that are observed in recorded signals, travel-time curves, contour maps, and in the associated diffraction

patterns. As the source-receiver positions or, in the phonon case, the source frequency, vary, the patterns change their morphologies according to typical universal bifurcation sets (caustics). These and the resulting universal power laws permit a reconstruction of profiles in a genuine zero-offset survey. The topological singularity and bifurcation concepts deriving from structural stability provide a unifying framework for all scattering techniques currently in use. The resulting conceptually simple processing methodology yields directly the desired end result of interpretation and comes much closer to the interpreter's intuitive qualitative approach than wave-equation based methods. Moreover, the topological singularities provide an explanation for the similarity and universality of the high-intensity patterns encountered in surface sensing [19], [20], [21], seismology [22], ocean acoustics [23], electromagnetic sensing [24], [25], ultrasound tomography, phonon spectroscopy [26], and so forth.

III.1. INVERSE SCATTERING

1. Wavefield singularities

Suppose a point source at $\underline{x}_o$ in space emits a spherical wave pulse that propagates through a layered medium made up of partially reflecting surfaces. The scattered wave $\psi(\underline{x}_o,t)$ that is received back at the source -- the echo -- exhibits as a function of time t a number of strong peaks which vary with the source position $\underline{x}_o$. In this echogram (a seismogram in a geological survey) caustic structures are discernible, e.g., those shown in Figure 8 where the intensity $|\psi|^2$ of the echo is plotted as a function of the (vertical) time or depth, and of the (horizontal) source position. Known as bright spots in seismology, these caustic events and the diffraction patterns around them are the singularities which the medium impresses on the sensing wavefield. They are at the root of the interpreter's intuitive geometric, i.e., qualitative, approach to remote sensing. Indeed, an interpreter readily points out that the layered medium which produces the echogram of Fig. 8 is the one shown in Fig. 9.

In discussing the effects of caustics we confine ourselves to a single reflecting surface. Since source and receiver are at the same place, only the geometrical optics specular reflection points of the surface whose distance vectors to the source are normal to the surface contribute to the echo. Then, as an observer at $\underline{x}_o$ moves along a line on an observation surface Σ above the surface, the reflecting point moves in the same direction for a surface with low curvature. But when the line is above the lowest curvature center of a concave part of the surface S, the reflecting point suddenly moves in the opposite direction. This reversal in direction occurs when $\underline{x}_o$ on Σ crosses the surface's evolute E (the set of loci of the surface's curvature centers). The evolute is the envelope of the surface normals where neighboring rays, normal to S, touch and focusing occurs (Fig. 10 a). When the source-receiver -- the shotpoint for short -- crosses E, then the number of rays going through $\underline{x}_o$ suddenly changes by two and so does the number of specularly reflecting points. This implies that the number of arrival peaks in the echo also changes by two.

Therefore, the reversals in the propagation direction of the specularly reflecting points, as seen from $\underline{x}_o$, are recorded as cusps in the echo profile (Fig. 10b). Indeed, while there is but one echo when $\underline{x}_o$ is at A, there are three when $\underline{x}_o$ is at B. Fig. 10b is revealed in Fig. 8.

In three-dimensional space the observation surface Σ intersects the evolute sheet generically in smooth curves L, called fold (A_2) lines, and in isolated cusp (A_3) points $\hat{C}$ (Fig. 11). As the height of Σ varies, the fold lines evolve into evolute sheets while the cusp points evolve into lines called ribs. If the rib is curved upwards (or downwards) and Σ is nearly tangent to a point on the rib, then the observation surface intersects the evolute in two beak-to-beak cusp singularities (or in a lip). This is shown in Fig. 12 for the winged evolute sheets E of a saddle-surface S. Let $R = R(\underline{x}_o, \underline{x}) = |\underline{x}_o - \underline{x}|$ be the distance from $\underline{x}_o$ to a point $\underline{x}$ on on S and $T = 2R/c$ the two-way travel-time (with speed c). The signals that are received back at the source after reflections by the specular points $\underline{x} = \underline{x}_s(\underline{x}_o)$ on S have travel-times

$T_s = T(\underline{x}_o, \underline{x}_s(\underline{x}_o))$ or distances $R_s = R(\underline{x}_o, \underline{x}_s(\underline{x}_o))$. These form a multi-sheeted 3-dimensional hypersurface in 4-dimensional $(T_s, \underline{x}_o)$-space. For example, in case of a plane observation surface Σ, with $\underline{x}_o = (x_o, y_o)$, the saddle-surface S of Fig. 11 gives rise to the travel-time surface on top of Fig. 12 with two-dimensional sections shown below.

A rib is smooth except for isolated points where either of the following singularities can occur: (i) the rib itself has a cusp point, called a swallowtail point (A_4) because near it the evolute has the shape shown in Fig. 4. (ii) a rib may touch a fold or two other ribs; in this case two evolute sheets have a contact in a common curvature center and are either hyperbolic or elliptic umbilics (D_4^+ or D_4^-) shown in Figs. 5 and 6, respectively, and the surface has an umbilic point. Since the observed singularities in echo recordings derive from the focal surfaces which constitute evolutes, and since still more complex caustic morphologies will arise if a surface possesses edges [27], [28], or if source and receiver are different [19], the question arises

how to classify the singularities a surface impresses on a sensing wavefield or ray family. To understand this, we need catastrophe theory [19] (Sec. II).

2. Structural stability of remote sensing

Let the point $\underline{x}$ on the smooth surface S be parametrized by surface coordinates $\underline{x} = \underline{x}(x,y)$. The distance vector $\underline{R}_s = \underline{x}_o - \underline{x}_s$ from a specular reflection point $\underline{x} = \underline{x}_s(\underline{x}_o)$ to the source is normal to S, $\underline{R}_s = R_s(\underline{x}_o)\underline{n}(\underline{x}_s)$ where $R_s = |\underline{x}_o - \underline{x}_s|$ (cf., Fig. 13 for the basic scattering geometry). The distance R has an extremum R_s at $\underline{x}_s$: $\underline{t}\cdot\nabla_{\underline{x}} R = 0$ for vectors $\underline{t}$ tangent to S, or

$$\nabla R = 0 \tag{3.1}$$

with $R = R(\underline{x}_o, \underline{x}(x,y))$ and $\nabla = (\partial/\partial x, \partial/\partial y)$. By definition, a solution $\underline{x} = \underline{x}_s(\underline{x}_o)$ of (3.1) is a stationary point, or a "topological singularity" of R. The type of singularity R possesses at $\underline{x}_s$ depends on the Hessian determinant

$$H(R) = \begin{vmatrix} R_{xx} & R_{xy} \\ R_{xy} & R_{yy} \end{vmatrix} \tag{3.2}$$

evaluated at $\underline{x}_s$. If $H \neq 0$, $\underline{x}_s$ is said to be nondegenerate. In this

case, R can be represented by a stable Morse quadratic form. If H=0, $\underline{x}_s = \underline{x}_{sc}$ is called a degenerate specular point. In that case $\underline{x}_o = \underline{x}_c$ lies in a curvature center $\underline{x}_c$ on the surface's evolute E. The equation for the evolute follows by eliminating x and y from (3.1) and H=0, leaving one equation for $\underline{x}_o = x_c$ alone.

At this point we require that the scattering process underlying remote sensing be structurally stable, i.e., that the observed images preserve their quality under slight perturbations of the system caused, e.g., by slight deformations of the surface or by small variations of the source. Then Thom's theorems [3] assert that -- in an appropriate curvilinear surface coordinate system denoted again by (x,y) and in a curvilinear source coordinate system $\underline{x}_o - \underline{x}_c = (u,v,w)$ -- the structurally stable distance function R can take on but five "catastrophe" polynomial normal forms near a degenerate specular point $\underline{x}_{sc}$ inside a smooth part of S, viz.,

$$R = R_o + P(x,y;\underline{x}_o) + Dy^2/2 \qquad (3.3)$$

where $R_o = |\underline{x}_c - \underline{x}_{sc}|$ and $D = \kappa_1 - \kappa_2$ where κ_i are the surface's principal curvatures in $\underline{x}_{sc}$. If $D \neq 0$, P is one of the cuspoid polynomials A_2 (fold): $P = x^3+ux$; A_3(cusp): $P = x^4+ux^2+vx$; A_4 (swallowtail): $P = x^5+ux^3+vx^2+wx$. If D=0, $P = xy^2 \pm x^3+wy^2+ux+vx$ represents the hyperbolic (D_4^+) resp. elliptic (D_4^-) umbilic polynomials. The bifurcation set of R is just the evolute E which, therefore, is classified into the five types mentioned above. They are shown in Figs. 3 (A_3), 4 (A_4), 5 (D_4^+) and 6 (D_4^-). As a consequence, there are but five structurally stable and generic travel-time singularities observable in an echogram. All others are concatenations of these. If source and receiver are at different positions, there are 14 genuine singularities [19], but the above five describe completely the observed high intensity focal surfaces. Their structural stability can be attributed to the fact that because of the high intensity accumulated in the caustics these are insensitive to small perturbations.

For A_3, Equ. (3.1) yields with (3.3) the equation $4x^3+2ux+v = 0$, i.e., the "overhanging cliff" of Fig. 2 where $v = -x_o$,

X = x and u = h are identified with the source position, surface point and height h of the observation line. Projecting the cliff's edges onto the (x_o,h)-plane gives a cusp which is precisely the evolute E of Fig. 10. A geometric interpretation of Fig. 2 in another context is given in Sec. II.

3. Travel-times, contour geometry and surface reconstruction

Structural stability implies that, as the source position varies, the travel-times change their morphologies according to universal bifurcation sets. The travel-times recorded in the echo as a function of the source position are obtained by eliminating x and y from the equations (3.1) and (3.3). One example is shown in Fig. 12. A bifurcation sequence of travel-times coming from an umbilical surface point of elliptic type, when $\underline{x}_o$ = u varies on a line above the curvature center, is shown in Fig. 14, where $\rho_s = R_s - R_o$. The spherical wavefronts of constant radius r=R, centered on $\underline{x}_o$, cut the surface in a series of contours $C(r,\underline{x}_o)$ (cf., Fig. 13). An observer moving with $\underline{x}_o$ sees the Fresnel-zone contour topography

changing according to universal bifurcation sets. A typical topographic change is shown in Fig. 15 for an umbilical surface point of hyperbolic type. The contours follow by setting $R-R_o=r=\text{const}$ in (3.3).

As the source-receiver $\underline{x}_o$ varies above the surface, each point of S eventually becomes specular. In virtue of the specularity condition (3.1), the surface normal at $\underline{x}_s$ is given by $\underline{n}(\underline{x}_s(\underline{x}_o)) = \nabla_{\underline{x}_o} R_s(\underline{x}_o)$. Then we obtain from $\underline{x}_o - \underline{x}_s = R_s\underline{n}$ the equation for the surface

$$\underline{x} = \underline{x}_o - R_s(\underline{x}_o)\nabla_{\underline{x}_o} R_s(\underline{x}_o) \qquad (3.4)$$

Since $|n|=1$, only two components of $\nabla_{\underline{x}_o} R_s$ are needed and it suffices therefore to vary $\underline{x}_o$ on a surface Σ, say, on a plane. Inferring R_s from the arrivals or peaks the echo ψ possesses at times $t=T_s=2R_s/c$, the surface profile can be reconstructed directly from (3.4). For an input signal F(t) with basic source pulse frequency ω_o (cf., Sec. 4), the echogram near a degenerate singularity $\underline{x}_s=\underline{x}_{sc}$ has the form

$$\psi(t,\underline{x}_c) \propto \omega_o^{\alpha}\{AF(t-T_{sc})+B\bar{F}(t-T_{sc})\} \qquad (3.5)$$

where $\alpha=\{1/6,\ 1/4,\ 3/10,\ 1/3\}$ for the singularities $\{A_2, A_3$

A_4, D_4^+} and $\bar{F}$ is the Hilbert transform of F. Varying ω_o and measuring the rate of change of the received power permits one to identify and to classify the structural details of the reflecting surface near travel-time reversals.

4. Diffraction Patterns

In classifying travel-times and surface contours the language of ray theory has been used so far. The wave-type diffraction patterns around the caustics follow from Kirchhoff's diffraction formula [19] for the backscattered wave ψ in the shortwave limit,

$$\psi(t,\underline{x}_o) = (1/8\pi^2 c)\int_o^\infty dr G(r,\underline{x}_o)\dot{F}(t-2r/c) \qquad (3.6)$$

with the incident spherical wave $F(t-R/c)/4\pi R$. Here, the surface structure function G -- the wavefront sweep velocity or scattering matrix -- is given by the integral

$$G(r,\underline{x}_o) = \int_S dS R^{-3}(\underline{n}\cdot\underline{R})\delta(r-R) = r^{-3}\int_{C'} ds\sqrt{|g|}(\underline{n}\cdot\underline{R})/|\nabla R| \qquad (3.7)$$

where δ is Dirac's function and the contour C' is the projection of C (Fig.13) onto the (x,y)-plane. From (3.7) the main contributions to G (and ψ) are seen to come from those values of r for which the integrand is infinite, i.e., from the geometrical optics specular reflection points given by $\nabla R=0$, Equ. (3.1). The Fourier transform of G is

$$\tilde{G}(k,\underline{x}_o) = \int_S dS(\partial R^{-1}/\partial n)\exp(ikR) \qquad (3.8)$$

where $k=\omega/c$. Hence, $\tilde{\psi}(\omega,\underline{x}_o)=-i\omega\tilde{G}(2\omega/c,\underline{x}_o)\tilde{F}(\omega)/8\pi^2 c$. The generic diffraction patterns associated with the travel-time singularities follow by substituting (3.3) into (3.8). Asymptotic evaluation of (3.8) gives high-intensity diffraction patterns of Airy, Pearcey and higher-order type [19,29]. The ω_o-dependence in (3.5) follows from (3.8) and (3.3) by scaling. A typical diffraction pattern around an elliptic umbilic caustic is shown in Fig. 16 (cf., also Fig. 8).

If the surface possesses edges and faults [27], the evolutes are amputated by the surface's shadow boundaries (Fig. 17). The effects produced by such discontinuities can be classified by six "constraint" catastrophe polynomials [30],[31]. For example, a fault (Fig.17) is determined by $P=x^3+vx^2+ux$ $(x>0)$ and the diffraction pattern following from (3.8) is of combined Fresnel-Airy type: The intensity near the travel-time reversal decreases much faster than the one produced by a slope. Figs. 18 (a) and (b) show the travel-time curves when $\underline{x}_o$ varies on a line above and below the point B in Fig. 17, respectively. This effect is also present in Fig. 9.

III.2. PHONON FOCUSING

The above classification of singularities in wavefields and ray families scattered back by a surface can be generalized to deal with inhomogeneous and anisotropic media [32] - [34]. Incorporating these topological concepts into S-matrix techniques of inversion offers new and practicable tools for all the sensing processes presently in use in a wide variety of physical and technical systems.

Perhaps the most beautiful and indeed unpredictable application of the above ideas arose when it was discovered that the topological principles just described also govern the remarkable phenomenon of focusing of ballistic phonons in condensed matter physics. The central idea is to create "ballistic heat pulses" in anisotropic crystals at low temperature so that a collisionless motion is made possible which dominates diffusive (thermal phonon) processes. Suppose a burst of heat energy is created at a point of a crystal surface with a laser or electron beam. The heat produces phonons radiating in all directions. For a single crystal cooled to low temperatures (2K) the phonons

travel in it ballistically, i.e., without scattering, at the speed of sound over distances of the order of centimeters. Since the elastic properties in a crystal are anisotropic, the constant-frequency (or energy) surface in wave-vector ($\underline{k}$-)space is in general not spherical and displays pronounced anisotropy depending on the material. Consequently, the group velocity v which defines the direction of the energy flux of the elastic (or phonon) wave, is also very anisotropic. The group velocity is normal to the constant-frequency surface S_ω and thus $\underline{k}$ and $\underline{v}$ are not colinear. Thus, considering an incoherent phonon source with isotropic angular distribution of $\underline{k}$-vectors, the phonon flux is channeled into intense beams along preferred crystal directions. This channeling of high-frequency phonons is called phonon focusing because time-integrated signals are detected as two-dimensional high intensity images exhibiting caustic effects. Singularity theory classifies the singular events which typically (generically) occur if the frequency which determines the frequency surface varies in a nonlinear dispersion relation. The changes in that surface induce the topological changes in the caustics. Again, the

reason for such a classification being possible is that the image produced by ballistic phonons must be insensitive to small perturbations in the system, i.e., structurally stable. Suppose a monochromatic point source of frequency ω generates phonons with wave-vectors $\underline{k}$ that propagate ballistically in a crystal whose anisotropy is described by a dispersion relation $\omega=\Omega(\underline{k})$. Then only those $\underline{k}$ contribute to the phonon field $u(\underline{r},\omega)$ at a point $\underline{r}$ in space which make up the constant-frequency surface $S=S_\omega:\omega=\Omega(\underline{k})$ = const, i.e.,

$$u(\underline{r},\omega) \propto \int d\underline{k}\,\delta(\omega-\Omega(\underline{k}))e^{i\underline{k}\underline{r}} = \int dS \frac{e^{ir\phi}}{|\nabla\Omega(\underline{k})|} \qquad (3.9)$$

for a given polarization mode. Here, $\underline{r}=r\hat{\underline{r}}$ with unit vector $\hat{\underline{r}},\phi=\hat{\underline{r}}\cdot\underline{k}$ and the second integral is taken over S. Suppose first that the phonon's group velocity $\underline{v}=\nabla\Omega(\underline{k})$, with $\hat{\underline{v}}=\underline{v}/|\underline{v}|=\underline{n}$ the unit normal to S, has no zeros. Then the phonon flux is in the directions $\hat{\underline{r}}=\hat{\underline{v}}(\underline{k})$. The corresponding wave-vectors $\underline{k}$ on S are (for large r) those for which ϕ is stationary, $\underline{t}\cdot\nabla_k\phi=0$ for vectors $\underline{t}$ tangent to S. Phonon focusing directions, i.e., angular caustics, come from the inflection points of S along a principal curvature line where the Gaussian curvature vanishes. These are the stationary points where the Hessian determinant of ϕ vanishes.

Since the caustics are structurally stable, i.e., insensitive to small perturbations, ϕ is equivalent to a Thom catastrophe polynomial $\phi=P$. This implies that the caustics can be classified by the topological singularities of the Gaussian map G of the frequency surface S on the multiply covered sphere S^2 of the group velocity directions $\hat{\underline{v}}(\underline{k})$ on which the caustic images are observed (Fig.19).

The fact that the structurally stable caustics are the images on S^2 of all points on S with zero Gaussian curvature has the following consequences. By Whitney's theorem, the only generic singularities on S^2 are folds and cusps. They are produced, respectively, by the line L on S with zero Gaussian curvature and its points of contact with the principal curvature line P that has zero curvature on L. When the fold lines, which separate dark from bright regions on S^2, are crossed, the number of phonon $\underline{k}$-vectors changes by two while three $\underline{k}$-vectors coalesce at a cusp point. If the dispersion relation is linear, $\omega=c(\hat{\underline{k}})k$ (nearest neighbor interaction), the surfaces S are similar for different ω, so that folds and cusps are the only possible caustics. If, however, the dispersion relation $\omega=\Omega(\underline{k})$ is non-

linear (long range forces), a variation of ω may change the topological type of S and that of the caustics when ω crosses a critical value ω_c. These sudden transitions are called critical events. Parametrizing G by $\omega-\omega_c$, the following events can occur.

(i) Swallowtail: Here, L has a second-order contact with P (Fig. 20b) which splits into three intersections (Fig.20a) and one intersection (Fig.20c) of L with P for $\omega<\omega_c$ and $\omega>\omega_c$, giving rise to the caustics of Fig. 21.

(ii) Hyperbolic and elliptic umbilics: S possesses an umbilic point which is a point $\underline{k}$ with equal principal curvatures where the surface is locally spherical. In the case of a hyperbolic umbilic the curvature vanishes for $\omega=\omega_c$ and the locally flat S produces the middle caustic in Fig.22b. For $\omega\gtrless\omega_c$, a tangential contact of L and P produces the cusps in the two other caustics in Fig.22b. An elliptic umbilic point appears when a circular L shrinks to a point for $\omega\to\omega_c$ from below and expands into another circle for $\omega>\omega_c$. The resulting caustic is shown in Fig.22a. The three cusps in Fig. 22a shrink to a point for $\omega\to\omega_c$.

(iii) There are but two possible degeneracies in a line L for $\omega=\omega_c$, viz., one that produces a caustic beak-to-beak event

(Fig.23a) and one giving rise to a caustic lip event (Fig.23b). These singularities exhaust all stable possibilities when no symmetries are involved. On a crystal's reflection planes and rotation axes new types of caustics are generated. They have been described in [34]. A C_6-symmetric singular event is shown in Fig.24. The Airy, Pearcey etc. diffraction patterns around the caustics follow by substituting P into (3.9) and evaluating the integral asymptotically [19]. By scaling one finds that on the caustic $|u|\propto r^{-\beta}$ for large r with the singularity indices $\beta=(5/6,\ 3/4,\ 7/10,\ 2/3)$ for the fold, cusp, swallowtail and umbilic events and $\beta=3/4$ for lips and beak-to-beak events.

If the dispersion relation $\omega=\Omega(\underline{k})$ has stationary (Morse) points, where the group velocity $\underline{v}$ vanishes, a new phenomenon springs up. Suppose that in Fig. 25 $(\omega_1,\underline{k}_1)$ is a minimum and $(\omega_2,\underline{k}_2)$ a saddle. Then the constant-frequency surface develops a second disconnected sheet when ω goes through ω_1, which gives rise to an overall flux enhancement. If ω goes through ω_2, the two surfaces coalesce in one of the two ways shown in Fig. 26. The caustic originating from the vertex of the cones is a great circle on S^2, but since $\underline{v}$ is zero at the point $\underline{k}_2$, the inten-

sity is zero and, therefore, this circle must appear as a dark ring ("anticaustic"). On either side of this dark line one expects two diffuse bright small circles whose positions correspond to the semiangles of the distorted cones near the vertex. We expect that with the recent development of tuneable phonon sources the caustic singularities occuring at the specific critical frequencies ω_c will become accessible to detailed experimental investigation. The same singularity-theoretical methods can be applied to photon focusing in anisotropic optics, magnon focusing and so forth. Similar focusing phenomena are well-known in magnetohydrodynamics. Finally it may be observed that the same caustics also dominate visual recognition processes in biophysics as they do in all optics.

IV. BIFURCATION GEOMETRY AND STRUCTURE FORMATION

This section addresses the topological problems posed by the formation of similar patterns and modes of behavior in physical systems whose order parameters or state variables undergo spontaneous changes if slowly varying and competing driving forces enter conflicting regimes by crossing a bifurcation set. The general physical situation has been discussed in paragraph two of the Introduction. Our objective is to describe and classify the transitions between possible configurations of solutions of nonlinear evolution equations by using normal forms of structurally stable families of maps in the framework of imperfect bifurcation theory (Sec. II).

Most of the nonlinear evolution equations of physics (e.g. the Bloch and Navier-Stokes equations) are not amenable to a quantitative analysis and few, if any, are completely known, so that it is often not clear for which particular effects one ought to look. Since these equations derive from general principles (conservation laws etc.), one wishes to find out which types of interacting time-periodic and steady-state solutions can occur under the hypothesis that they are structurally stable,

i.e., that they preserve their quality under slight perturbations. A system of general evolution equations depending on a control parameter λ and a set of imperfection parameters σ can be reduced (e.g., by the Lyapunov-Schmidt method) to a small number of algebraic equations for the amplitudes of the stationary solutions and the amplitudes of the time-periodic solutions. These are the bifurcation equations of the system. Solving them would give a complete picture of the spatio-temporal structures and modes of behavior of the system. Unfortunately, they can be solved just as little as the original evolution equations themselves. However, one can perform a change of coordinates in such a way that, in the new variables, the bifurcation equations reduce to simple polynomial normal forms. The latter can be classified and play the role of "organizing centers" in which all the degenerate singularities responsible for instabilities of the system are compressed. Perturbing them reveals all possible bifurcations which are stable against imperfections and so can occur generically in evolution problems of whatever genesis. Two types of bifurcation of solutions of general evolution equations are fundamental: The bifurcation of a steady

state with amplitude x and the Hopf bifurcation of a time-periodic solution with amplitude y from a stationary one. Interactions between them lead to secondary bifurcations of periodic solutions and to tertiary bifurcations of double-periodic motions lying on tori and eventually to chaotic motions. This interaction occurs if a control parameter λ crosses some critical values. Imagine, e.g., that x and y satisfy two algebraic normal form equations $a(x,y^2,\lambda)=0$ and $b(x,y^2,\lambda)=0$. The solution of the first is a two-dimensional multisheeted surface $y=\phi(x,\lambda)$ in (x,y,λ)-space, that of the second equation is another surface $y=\psi(x,\lambda)$. The lines along which both surfaces intersect give the simultaneous solutions of both equations, i.e., the bifurcation set of the evolution equation from which the behavior of the system can be inferred as λ varies. The intersection of the two surfaces may either be transversal so that any slight deformation of the surfaces causes no new types of intersections: Structural stability of the bifurcation diagram is ensured. However, if the two surfaces intersect with tangential contact (organizing centers), or just touch, then a slight deformation of them produces new

intersections and so gives rise to new bifurcation possibilities which then, however, are stable aginst any further perturbations. These deformations can be thought to be induced by variations of the imperfection parameters in the original evolution equations. Since the forms of the perturbed polynomials a and b and the surfaces they determine can be classified into a finite set, the problem of interacting spatial and temporal patterns has thus been reduced conceptually to a concatenation of possible basic bifurcation diagrams. In other words, by requiring structural stability of a system, its generic modes of behavior can be inferred from universal (i.e., topologically invariant) geometrical structures. All that has to be done is to determine the rules according to which the diagrams can be connected (different from but akin in spirit to Feynman rules). This program is presently being executed, but it is fair to admit that we are only at the beginning of an emerging "geometrization of physics". Still, already at the present stage, the predictive power of this sort of reasoning is quite surprising.

In this section the above arguments are applied to classify interacting Hopf and steady-state bifurcations which can generically occur in autonomous nonlinear evolution equations with a distinguished external control parameter and a set of system-immanent imperfection variables. A variety of new phenomena, such as gaps in Hopf branches, periodic motions not stably connected to steady states, and the formation of islands are discovered which one can expect to find in evolution equations on pure geometric grounds. The results are discussed in detail in [35] and are based on those of a highly mathematical paper [12] in which symmetry-covariant imperfect bifurcation equations for systems with two order parameters have been classified and organizing centers have been determined. The physical significance of these findings is that the sudden transitions between spatial and temporal patterns, which occur when parameters vary, are independent of the underlying particular mechanisms. The theory has been applied in [35] to the Brusselator model of chemical reactions and it was shown that this model describes a variety of new phenomena that have so far not been anticipated. Perhaps the most fascinating new physical result sprang

up in [36], where the above ideas were applied to the problem of self-pulsing in optically bistable systems, which carry great potential for technical applications. Here, an organizing center for all possible bifurcations, giving rise to new phenomena of self-pulsing from the low transmission branch and island formation, was discovered. The new phenomena, predicted on topological grounds alone, still await experimental confirmation.

IV.1. INTERACTING HOPF AND STEADY-STATE BIFURCATIONS

1. Bifurcation Equations

Suppose that the dynamics of a physical system are governed by the system of evolution equations

$$\frac{\partial v}{\partial t} = F(v,\lambda) \qquad (4.1)$$

where v is an element of an appropriate Banach space, $\lambda \in \mathbb{R}^1$ is a real bifurcation parameter, and F is a smooth nonlinear operator defined on a neighborhood of the origin and satisfying $F(0,0)=0$. We assume that the linearized operator

$$A = D_v F(0,0) \qquad (4.2)$$

has a simple zero eigenvalue and, in addition, a simple pair of imaginary eigenvalues $\pm i\omega_o$ ($\omega_o > 0$). The remaining spectrum of A is assumed to be to the left of the imaginary axis. The problem we are concerned with is the following. Equation (4.1) has the stationary solution $v=0$ for $\lambda=0$. When the externally controllable bifurcation parameter λ is varied away from zero, then, because of the nonlinearity of F, two basic types of solutions bifurcate from the trivial one, viz., (i) steady-state solutions associated with the zero eigenvalue (e.g., limit point bifurcations and hysteresis), and (ii) time-periodic or Hopf solutions associated with the eigenvalues $\pm i\omega_o$ of A. The nonlinearity of F causes these two solutions to interact and, since they tend to the trivial solution $v=0$ for $\lambda \to 0$, F has a degenerate bifurcation at $(0,0)$. The degeneracy can be removed by subjecting F to small perturbations, representable, e.g., by additional imperfection parameters σ in F itself, $F \to F_\sigma$. This is achieved by stably unfolding the algebraic bifurcation equations to which (4.1) will be reduced. Then, as the unfolding parameters are varied, zero and imaginary eigenvalues occur for different values of the

distinguished parameter λ and, with the degeneracy so removed, new bifurcation phenomena are springing up which are structurally stable.

Since the linearization of (4.1) at (0,0) has $(2\pi/\omega_o)$-periodic solutions, we seek for periodic solutions of (4.1) near (0,0) with period $2\pi/\omega$ where ω is close to ω_o. Setting $s=\omega t$, $u(s)=v(s/\omega)$ so that u has period 2π in s, we rewrite (4.1) as the nonlinear operator equation

$$N(u,\lambda,\tau) \equiv \tau\frac{du}{ds} + Lu - R(u,\lambda) = 0 \qquad (4.3)$$

where $\tau=\omega-\omega_o$, $L=\omega_o\frac{d}{ds}-A$ and $R(u,\lambda)=F(u,\lambda)-Au$. In the space E of (2π)-periodic vector-valued functions $u=u(s)$ the linear operator L has a three-dimensional nullspace spanned by the eigenfunctions $\phi=(\phi_1,\phi_2,\phi_3)$. In order to reduce the bifurcation problem (4.3) to an algebraic one by the Lyapunov-Schmidt method one decomposes

$$u = u(s,z) = \sum_{i=1}^{3} z_i\phi_i + w \equiv z\phi + w(s) \qquad (4.4)$$

with amplitudes $z=(z_1,z_2,z_3)$ and $\langle w,\phi_i\rangle=0$. Hence, $z\phi=Pu$ and $w=Qu$ with the projections $Pu = \sum_{i=1}^{3}\langle u,\phi_i^*\rangle\phi_i$, $Q=I-P$. Then,

solving (4.3) is equivalent to solving the two equations $PN=0$ and $QN=0$.

By standard implicit function arguments $QN=0$ has a smooth unique solution $w(z,\lambda,\tau)$, $w=o(z^2)$ which, when substituted into $PN=0$, yields the bifurcation equations

$$g_i \equiv \langle -\tau\frac{d}{ds}(z\phi+w) + R(z\phi+w,\lambda),\phi_i^*\rangle = 0 \qquad (4.5)$$

Equs. (4.5) express the fact that, for (4.3) to be solvable, R must be orthogonal to the eigenfunctions of L (Fredholm alternative). Since (4.1) is invariant under time-translation, it suffices to choose $z_2=0$. Therefore, solving $g_2=0$ for $\tau=\tau(x,\lambda,y^2)$ and substituting into the remaining two equations, (4.5) reduces to the degenerate algebraic system of bifurcation equations

$$G(x,\lambda,y) := \begin{pmatrix} a(x,\lambda,y^2) \\ yb(x,\lambda,y^2) \end{pmatrix} = 0 \qquad (4.6)$$

with

$$\begin{aligned} a(0,0,0) = b(0,0,0) &= 0, \\ a_x(0,0,0) &= 0 \end{aligned} \qquad (4.7)$$

The solutions of (4.6) are in one-to-one correspondence with those of (4.3). Therefore, the algebraic system (4.6) describes the Z(2)-equivariant interaction between the periodic (Hopf) solutions of Equ. (4.1) with amplitude $y \geq 0$ and the steady-state solutions with amplitude x when the bifurcation parameter λ varies. We classify and analyse these interaction phenomena in the next subsection.

2. Classification

The multivalued solutions of (4.6) are the bifurcation diagrams in (x,λ,y)-space. We classify them together with their stable perturbations by means of imperfect bifurcation theory (Sec. II), referring to [9], [35] for technical details.

Equ. (4.6) possesses two coupled types of solutions, viz., pure steady-state solutions with amplitude x determined by $\{a(x,\lambda,0)=0, y=0\}$, and periodic solutions with $y \neq 0$ obtained by the simultaneous solution of the equations

$$a(x,\lambda,y^2) = 0, \quad b(x,\lambda,y^2) = 0. \tag{4.8}$$

The periodic solutions may branch from the steady-state at

a secondary Hopf bifurcation point and may further undergo tertiary bifurcations to tori [35], [37]. Our approach to this problem is based on two central principles of topologically invariant bifurcation theory. The first is to change coordinates so that the qualitative topology of the bifurcation diagram $G=0$ is preserved, the special role of the externally controllable bifurcation parameter λ is respected and G takes a simple polynomial form from which the solutions may easily be determined. This problem is solved by using the notion of (Z(2)-equivariant) contact equivalence (Sec. II and [9]) of singularity theory which shows that, under certain conditions on the Taylor expansion of G (resp., F) at the origin, G is equivalent to one of the polynomial normal forms of corank two given in Table 1 of [12] and [35]. The second principle is to determine and to classify all the possible, stable and inequivalent, i.e., qualitatively different, bifurcation diagrams that may arise when a given $G(x,\lambda,y)$ is subjected to small perturbations which correspond to imperfections in F. This is achieved by using

the basic concept of singularity theory [9], [35], viz., the existence of universal unfoldings which capture all families of perturbations of G which, up to contact equivalence, preserve the distinguished role of λ -- distinct from the parameters determining perturbations. In bifurcation theory the unfolding problem goes under the name of imperfect bifurcation because of the sensitivity of a bifurcation diagram representing a physical phenomenon against internal imperfections. These may be interpreted as additional parameters in $F(v,\lambda)$ whose role is taken over by the unfolding parameters of a universal unfolding of G. Their number, the contact codimension of G, is a measure for the degree of complexity of the degeneracy. The complete degeneracy of (4.1), due to the zero and imaginary eigenvalues of $D_v F(0,0)$, implies that the solutions of the bifurcation problem are not structurally stable, i.e., they do not preserve their quality under slight perturbations of G. Embedding G into a stable family of unfoldings allows one to characterize this instability. Conversely, G can be considered as an organizing

center, i.e., as an idealized system in which all singularities any unfolding of G can possess are pushed together. Unfolding this highly singular configuration will then display the effects of all imperfections.

3. Bifurcation geometry

We present here a few generic perturbed bifurcation diagrams describing interacting Hopf (H) and steady-state problems (S), referring to [35] for a comprehensive study. Of major interest for applications are special points in the perturbed bifurcation diagrams, viz., limit points and secondary bifurcation points (SB) which are here all Hopf bifurcation points, and tertiary bifurcations (T) from the Hopf branch to a torus. The stability properties are indicated by assigning to each branch of a diagram its stability symbol ((--) stable, etc.), i.e., the signs of the real parts of the eigenvalues of the Jacobian DG.

In Fig. 27 we show the simplest secondary bifurcation (SB) of a Hopf branch (H) from a steady state in the (x,λ)-plane

associated with the normal form $(1)_{21}$: $a=x^2+\varepsilon_2 y^2+\lambda=0$, $b=y(x-\gamma)=0$. Figure 28 shows two Hopf branches bifurcating from a steady-state with bistability. In Figure 29 a tertiary bifurcation point T appears where a transition to a double-periodic solution occurs. There are many more diagrams exhibiting a variety of new phenomena such as gaps in Hopf branches, hysteresis between Hopf and steady-state branches, periodic solutions coming "out of nothing," i.e., not connected to steady states, and so forth. Their significance in a variety of physical systems, e.g., in Prigogine's Brusselator and in the Benard problem of hydrodynamics are presently in the center of interest [35]. As an example we discuss briefly the problem of optical bistability.

IV.2. OPTICAL BISTABILITY AND SELF-PULSING

Optically bistable systems are currently attracting increasing interest, not only because of their potential applications but also as laboratories for the study of nonlinear synergetic phenomena which exhibit multistability,

self-pulsing, interacting spatio-temporal patterns and chaotic behavior [38]. Since the Maxwell-Bloch equations which govern optical bistability cannot be solved analytically except in limiting cases, a geometrical approach along the lines sketched above appears necessary. That this is also feasible has recently been demonstrated [39]. By a reinterpretation of known numerical facts, one can find a degenerate self-pulsing situation on the high-transmission branch, which in virtue of structural stability leads to new bifurcation diagrams. Among them are first and second order transitions to the self-pulsing mode and the formation of an isola. Evidence is given for the existence of a cod 4 organizing center (cf. II) which organizes both the bistable switching (which itself is organized by a hysteresis point) and the self-pulsing whose degeneracy is an H(7) degenerate [9] Hopf-bifurcation. Unfolding this organizing center shows, apart from all known interaction phenomena, several new ones whose experimental or numerical detection is to be expected.

In optical bistability experiments a coherent laser beam is injected into an optical resonator (Fabry-Perot interferometer)

filled with a homogeneously broadened two-level atomic system between two partially transmitting mirrors within a feedback loop. The refraction index of the medium depends on the incident intensity I which plays the role of an externally controllable parameter λ, $I=\lambda$. The transmitted intensity x becomes a nonlinear function of I described by the S-shaped hysteresis loop of Fig. 30. Jumps from the high to the low transmission branch and vice versa describe the phenomenon of optical bistability. It has been shown that for pure absorption a section of the upper branch of the hysteresis curve can become unstable (the (+-)-part in Fig. 30). Then the system exhibits a limit cycle, i.e., an undamped time-periodic sequence of pulses branches from a cw-transmission. This is the Hopf bifurcation producing self-pulsing in optically bistable systems. We represent the amplitude of this time-periodic solution by y. Furthermore, there exists a region for the cavity mistuning and atomic detuning and values for the cooperation parameter such that the hysteresis curve can possess a point with a vertical tangent (a hysteresis

point). Consequently there are two degeneracies, viz., a hysteresis point in the stationary transmission branch and a degenerate Hopf bifurcation point on the upper branch. The simplest normal form $G(x,\lambda,y)$ in which both degeneracies coalesce is the form $(5)_{32}$, [39], viz.,

$$G = \begin{pmatrix} x^3 + y^2 - \lambda + \beta x + \alpha \\ y(x^2+\lambda^2) + y(\delta+\gamma x) \end{pmatrix} \qquad (4.9)$$

with unfolding parameters $\alpha,\beta,\gamma,\delta$ which depend on the system parameters. G is an organizing center for optical bistability bifurcations. The bifurcation diagrams of G=0 have been discussed in [15]. Some of these are shown in Figure 30 in which the loops emerging from the hysteresis curve are projections onto the (x,λ)-plane of the branches in (x,λ,y)-space. Among the new phenomena which one expects to find in optical bistability experiments are the following: Bifurcation to self-pulsing from the high transmission branch (Fig. 30.2); two hysteresis loops between self-pulsing and the cw-regime (Fig. 30.6), i.e., periodic motions not stably connected to a stationary solution; torus bifurcation points (marked by T or

dots on the loops of Fig. 30) which may lead to chaotic behavior. Perhaps the most surprising phenomenon to be encountered is the appearance of a stable island representing a self-confined light-pulsing that is trapped between fixed incident intensities (Fig. 30.7).

The phenomena just described still require experimental confirmation. Their theoretical existence has been proven on pure geometric grounds under the hypothesis that optical bistability is a structurally stable phenomenon. Let us briefly comment on chaotic behavior of optically bistable systems. Computer simulations indicate a Feigenbaum sequence to chaos [41] through period-doubling in optically bistable systems [38]. In addition a Ruelle-Takens scenario [40] may take place when the 2-torus T turns into a 3-torus by another Hopf bifurcation, thus leading to a strange attractor. In the present case another non-Feigenbaum route to chaos might spring up: It is known that a 2-torus is not structurally stable under perturbations breaking the SO(2) symmetry [42] but leads to transverse homoclinic orbits in whose

neighborhood chaotic behavior takes place. Such unstable tori also arise when two simultaneous Hopf bifurcations emerge from a point on the steady-state curve and interact. It would be interesting to discover such non-Feigenbaum routes to chaos in optically bistable systems.

V. CONCLUSIONS

We may summarize our results as follows. Both at the microscopic and macroscopic levels, the topological singularities and universal bifurcation processes deriving from the principle of structural stability of physical systems play together the decisive role in structure formation and structure recognition. These concepts are at the origin of all the geometric analogies discovered in the critical behavior of systems of different genesis which synergetics aims at describing. I have tried to illustrate the breadth of the impact of Thom's work by giving a brief selection from the many applications of bifurcation theory. Recent developments address problems in solidification and melting systems, fluid dynamics, chemical reactions, symplectic geometry and Lagrangian singularities and so forth. The next step ought to consist of incorporating singularity theory into particle physics and cosmology. In this context M. Schönberg's work on quantum mechanics and geometry appears to be of great significance. This problem raises very difficult but fascinating questions that promise a great challenge for future research.

ACKNOWLEDGEMENTS

It is both a privilege and a pleasure to dedicate this paper to Professor Mario Schönberg, senior of Brazil's theoretical physics, colleague and friend. It is also a perfect occasion to appreciate the insights I gained in the 1950's from him and from his pioneering contributions towards a geometrization of physics. In pursuing this goal further I thank D. Armbruster, G. Dangelmayr, Ch. Geiger, P. Haug, D. Lang, M. Neveling and F. J. Wright for their collaboration and the Stiftung Volkswagenwerk for the support of this research.

REFERENCES

[1] G. Nicolis and I. Prigogine: Selforganization in non-equilibrium systems (Wiley 1977).

[2] H. Haken: Synergetics (2nd Edition, Springer 1982) and Advanced Synergetics (Springer 1983).

[3] R. Thom: Structural Stability and Morphogenesis (Benjamin 1975).

[4] T. Poston and I. Stewart: Catastrophe Theory and Applications (Pitman, London, 1978). I. Stewart: Physica 2D (1981), 245-305.

[5] E. C. Zeeman: Catastrophe Theory (Addison-Wesley 1977). R. Gilmore: Catastrophe Theory (Wiley 1981).

[6] M. V. Berry: Les Houches Lectures 1980.

[7] W. Güttinger and H. Eikemeier (Eds.): Structural Stability in Physics (Springer 1979).

[8] V. I. Arnold: Mathematical Methods of Classical Mechanics (Springer 1978).

[9] M. Golubitsky and D. Schaeffer, Comm. Pure Appl. Math. 32 (1979) 21-98. M. Golubitsky and W. F. Langford: J. Diff. Equs. 41 (1981), 375-415. D. G. Schaeffer and M. Golubitsky; Arch. Rat. Mech. Anal. 75 (1981), 315-347.

[10] M. Golubitsky and D. Schaeffer: Comm. Math. Phys. 67 (1979), 205-232.

[11] D. H. Sattinger: Bull. Am. Math. Soc. 3, 779 (1980).

[12] G. Dangelmayr and D. Armbruster: Proc. London Math. Soc. 46 (3), 517 (1983).

[13] M. Golubitsky, B. L. Keyfitz and D. Schaeffer: Comm. Pure Appl. Math. 34 (1981), 433-463.

[14] I. S. Labouriau: Applications of Singularity Theory to Neurobiology (Univ. of Warwick preprint 1983).

[15] D. Armbruster: Z.Phys.B. 53, 157 (1983).

[16] Ch. Geiger and W. Güttinger: in preparation (1984).

[17] D. Armbruster and W. Güttinger: in preparation (1984).

[18] G. Dangelmayr: J.Phys.A. L337-342 (1982).

[19] G. Dangelmayr and W. Güttinger: Geophys. J. Roy. Astro. Soc. 71, 79 (1982).

[20] W. Güttinger and F. J. Wright: Topological Approach to inverse scattering in remote sensing, NATO-ARW proceedings (Reidel 1984).

[21] W. Berry: J.Phys.A 5, 272 (1972); F. J. Hilterman: Geophysics 40, 745 (1975).

[22] N. Bleistein and J. Cohen: US Nav. Res. Rep. MS-R-7806 (1978).

[23] J. B. Keller and I. Papadakis: Wave Propagation and underwater acoustics (Springer 1977).

[24] H. Baltes: Inverse Scattering in Optics (Springer 1980).

[25] W. M. Boerner in [24].

[26] H. Eisenmenger, K. Laßmann and S. Döttinger (Eds.): Phonon Scattering in Condensed Matter (Springer 1984).

[27] J. Achenbach and A. Norris: J. Acoust. Soc. Am. 70, 165 (1981).

[28] F. J. Wright: preprint (1984), see also [20].

[29] M. V. Berry and C. Upstill in E. Wolf (Ed.): Progress in Optics 257 (1980).

[30] T. Poston and I. Stewart in [4].

[31] F. J. Wright in [28], G. Dangelmayr and W. Güttinger in [19].

[32] J. P. Wolfe: Phys. Today 33, 44 (1980).

[33] P. Taborek and D. Goodstein: Solid State Comm. 33, 1191 (1980). Cf. also Ref. [26].

[34] D. Armbruster and G. Dangelmayr: Z.Phys.B 52, 87 (1983). D. Armbruster, G. Dangelmayr and W. Güttinger in [26].

[35] D. Armbruster, G. Dangelmayr and W. Güttinger: "Imperfection Sensitivity of interacting Hopf and Steady-State Bifurcations and their Classification", Physica D (1984) in print.

[36] D. Armbruster in Ref. [15].

[37] J. Guckenheimer and P. Holmes: Nonlinear Oscillations, Dynamical Systems and Bifurcations of Vector Fields (Springer 1983).

[38] R. Bonifacio (Ed.): Dissipative Systems in Quantum Optics (Springer 1982).

[39] See Ref. [15] and [12].

[40] F. Takens: Publications of the Institute des Hautes Etudes Scientifiques, Bures-sur-Yvette, Paris 43 (1974) 47-100, "Singularities of vector fields".

[41] J. P. Eckmann, Rev.Mod.Phys. 53 (1981) 643-654. E. C. Zeeman, in New Directions in Applied Mathematics, Case Western Reserve University 1980.

[42] J. Guckenheimer: SIAM J.Math.Anal. 15, 1(1984).

FIGURE CAPTIONS

Fig. 1 Pitchfork bifurcation

Fig. 2 Cusp catastrophe manifold

Fig. 3 Cusp

Fig. 4 Swallowtail

Fig. 5 Hyperbolic umbilic

Fig. 6 Elliptic umbilic

Fig. 7 Perturbed pitchfork

Fig. 8 Echo recording (seismogram)

Fig. 9 Layered medium which produces Figure 8

Fig. 10 (a) Surface and evolute, (b) Travel-time recording

Fig. 11 Saddle surface S, with evolute E

Fig. 12 Travel-time surface for Figure 11

Fig. 13 Surface geometry

Fig. 14 Travel-time bifurcation sequence from an elliptic umbilic surface point

Fig. 15 Contour map for a hyperbolic surface point

Fig. 16 Diffraction pattern around an elliptic umbilic

Fig. 17 Surface with a fault

Fig. 18 Travel-times produced by a fault

Fig. 19 Phonon focusing

Fig. 20 Curvature lines

Fig. 21 Swallowtail caustics

Fig. 22 (a) Hyperbolic and (b) elliptic umbilic caustics

Fig. 23 (a) Beak-to-beak event, (b) lip event

Fig. 24 Caustics in a crystal with C6 symmetry

Fig. 25 Nonlinear dispersion relation

Fig. 26 Caustic cones produced by a nonlinear dispersion relation

Fig. 27 Secondary Hopf bifurcation (SB) from a steady state

Fig. 28 Simultaneous Hopf bifurcation originating at a hysteresis branch

Fig. 29 Hopf-steady-state interaction leading to a torus point T

Fig. 30 Self-pulsing and island formation processes (from [15])

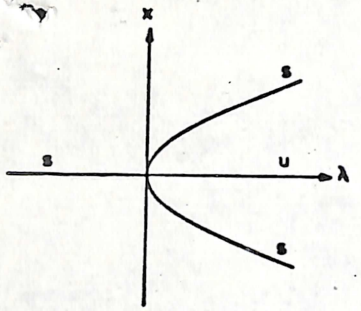

Fig. 1

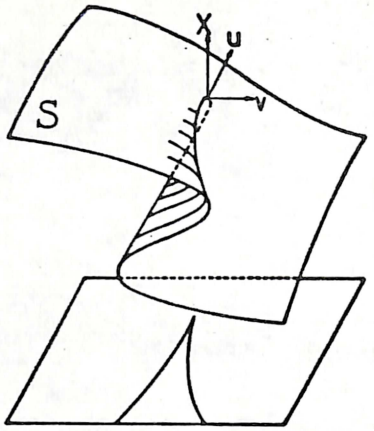

Fig. 2

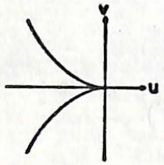

Fig. 3

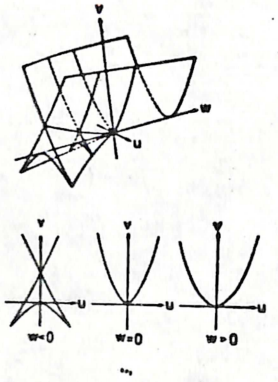

Fig. 4

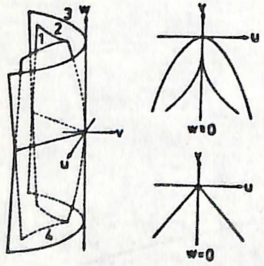

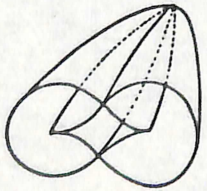

Fig. 5

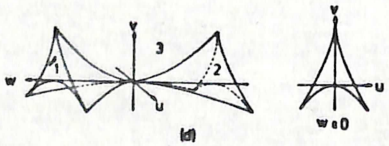

Fig. 6

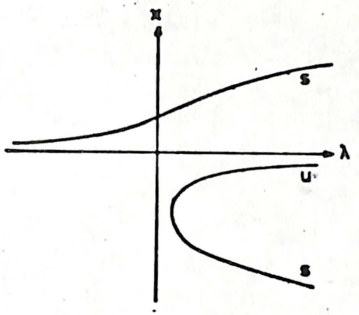

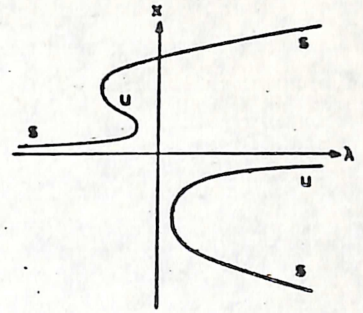

Fig. 7

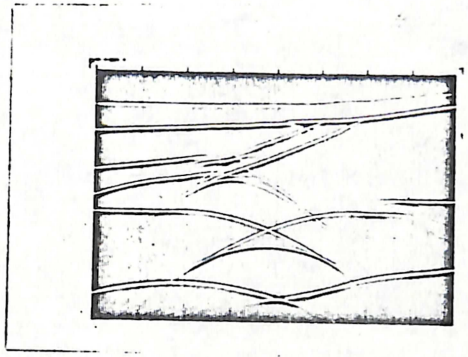

Fig. 8

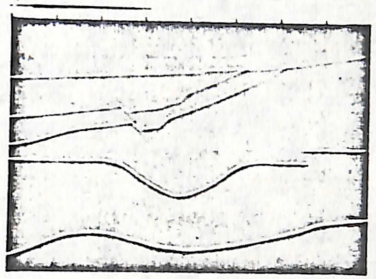

Fig. 9

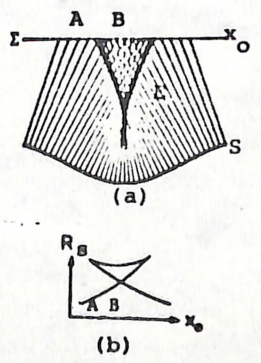

Fig. 10

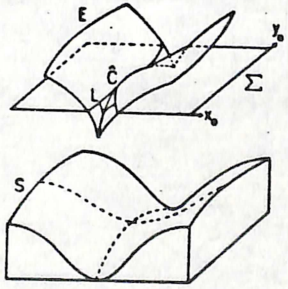

Fig. 11

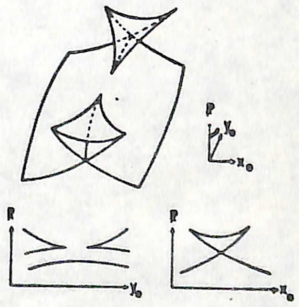

Fig. 12

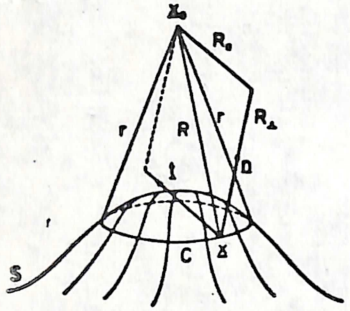

Fig. 13

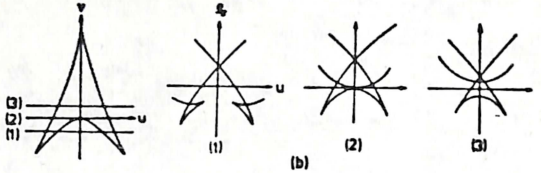

Fig. 14

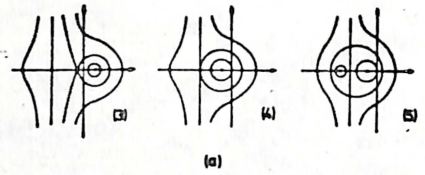

Fig. 15

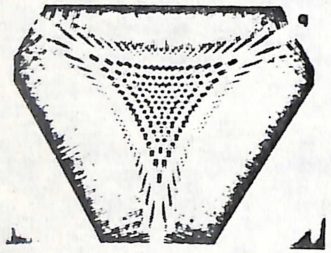

Fig. 16

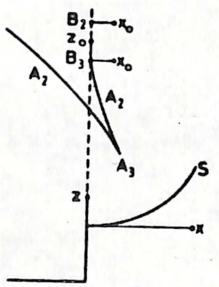

Fig. 17

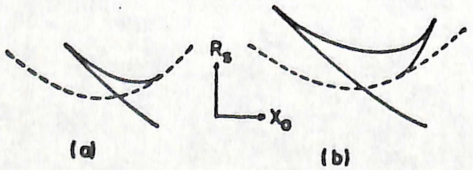

Fig. 18

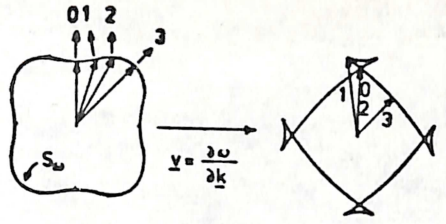

Fig. 19

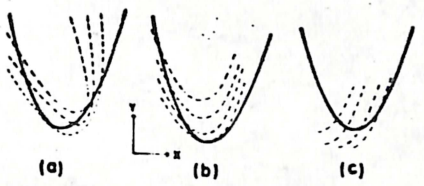

Fig. 20

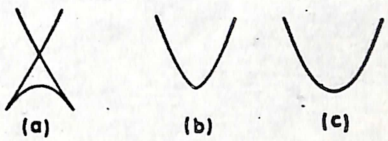

Fig. 21

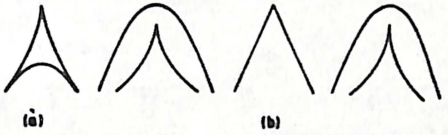

Fig. 22

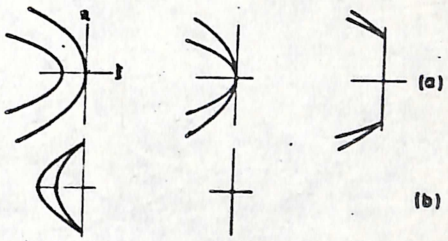

Fig. 23

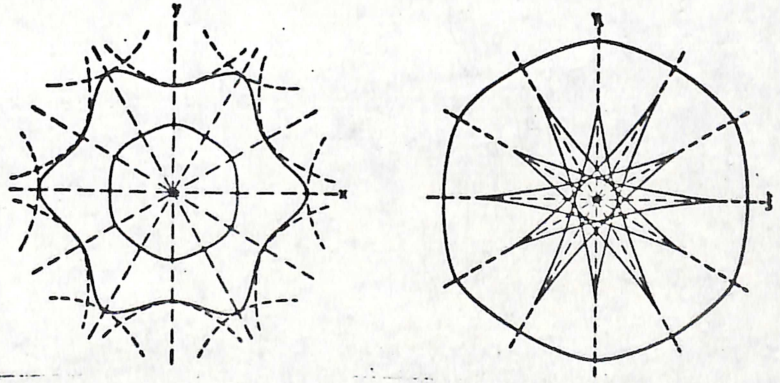

Fig. 24

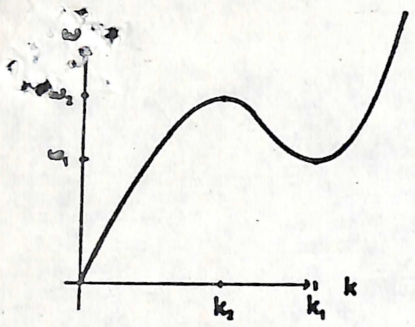

Fig. 25

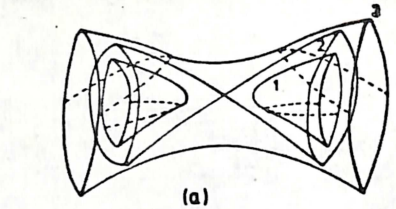

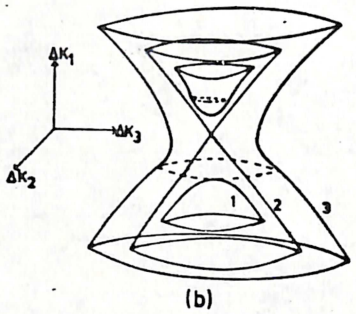

Fig. 26

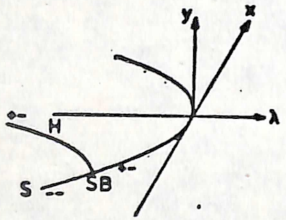

Fig. 27

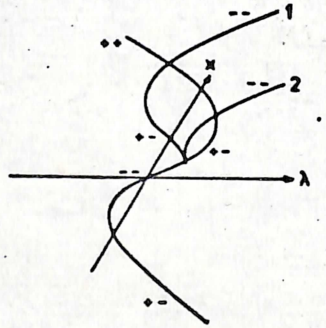

Fig. 28

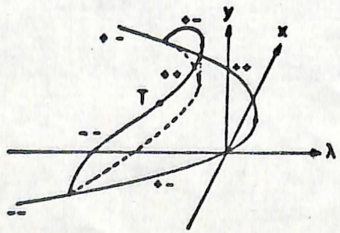

Fig. 29

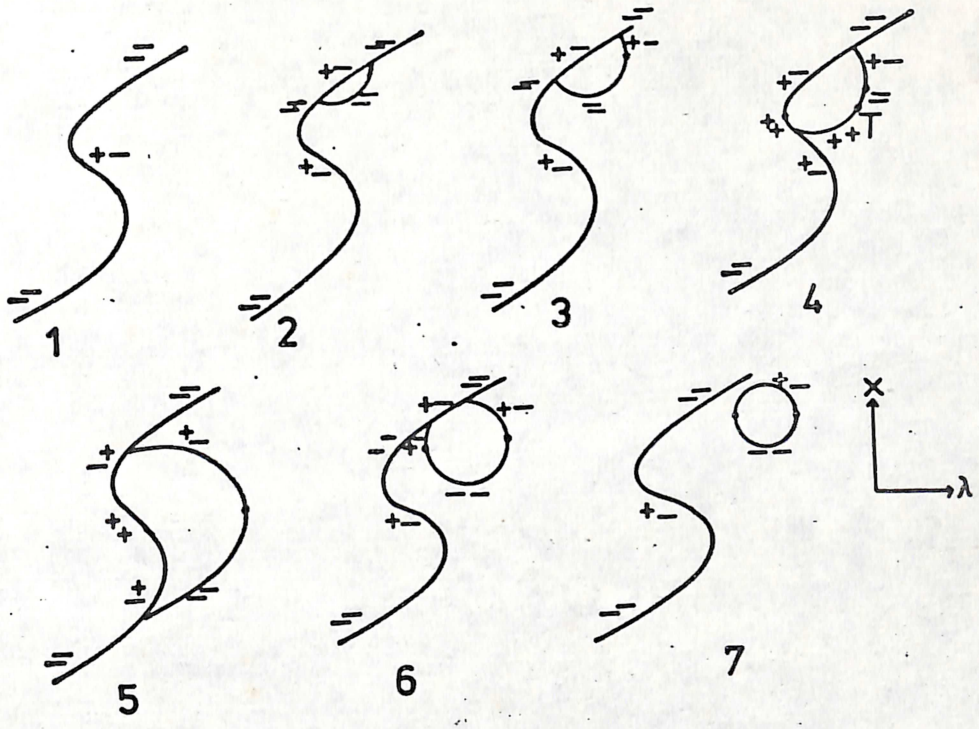

Fig. 30